Microstructure and mechanical properties of spark plasma sintered nanocrystalline Ni_3Al-xB (0.0<x<1.5 at%) alloy

Mohammadnejad, A.; Bahrami, A.; Sajadi, M.; Karimi, P.; Fozveh, H. R.; Mehr, M. Yazdan

DOI
10.1016/j.mtcomm.2018.09.002

Publication date
2018

Document Version
Final published version

Published in
Materials Today Communications

Materials Today Communications 17 (2018) 161–168

Contents lists available at ScienceDirect

Materials Today Communications

journal homepage: www.elsevier.com/locate/mtcomm

Microstructure and mechanical properties of spark plasma sintered nanocrystalline Ni_3Al-xB ($0.0 < x < 1.5$ at%) alloy

A. Mohammadnejad[a], A. Bahrami[a], M. Sajadi[a], P. Karimi[a], H.R. Fozveh[a], M. Yazdan Mehr[b,*]

[a] Department of Materials Engineering, Isfahan University of Technology, Isfahan 84156-83111, Iran
[b] Faculty EEMCS, Delft University of Technology, Mekelweg 4, 2628 CD Delft, The Netherlands

ARTICLE INFO

Keywords:
Ni_3Al intermetallic
Spark plasma sintering
Mechanical alloying
Nanostructure

ABSTRACT

This study aims at studying the microstructure and mechanical properties of nanocrystalline Ni_3Al-xB ($0.0 < x < 1.5$ at%) alloy, made by mechanical alloying (MA) and spark plasma sintering (SPS). Effects of milling time as well as boron addition on the crystallite size, lattice strain, and powder morphologies of synthesized powders were studied using scanning electron microscope (SEM) and X-ray diffractometer (XRD). Synthesized powders were consolidated under uniaxial compression 50 MPa at 950 °C for 10 min. Shear punch and hardness tests were used to evaluate mechanical properties of consolidated specimens. Results show that Ni_3Al compound were synthesized after 30 h of milling in a planetary ball mill with the rotation speed of 350 rpm and ball-to-powder ratio 10:1. Synthesized powders have crystallite size in the range 15–20 nm depending on the milling time. Results also show that boron addition is influential the most when boron content is between 0.5–1.0 at%. Boron addition is accompanied with a significant improvement of hardness and shear strength and a drop in the ductility of Ni_3Al-xB ($0.0 < x < 1.5$ at%) alloy. The details concerning structure-properties relationship in this system are discussed in this paper.

1. Introduction

Current demands for materials with superior high temperature properties have led many industries to start using high temperature heat resistant intermetallic compounds [1]. Amongst different available intermetallic alloys, Ni_3Al is believed to be a very good one, owing to the fact that it comprises a unique set of properties including very good high temperature mechanical properties, superior high temperature corrosion and oxidation resistance, and microstructural stability during service [2–4]. However, the application of this intermetallic compound is still very limited, partly due to its low ductility at room temperature, compared to superalloys and other heat resistant austenitic materials [5–7]. This obviously has negative implications for the application and manufacturing of components from this intermetallic, i.e. casting and metal forming of Ni_3Al components are difficult and expensive. Loads of attempts have been made in last two decades to enhance mechanical properties of Ni_3Al intermetallic compounds [8–10], by changing the process and the chemistry of the alloy. Amongst different proposed methods, powder metallurgy (PM)-based techniques offer more flexibility and are in fact currently widely used for manufacturing of Ni_3Al components with complicated geometries. The first step in any powder metallurgy-based manufacturing route, is synthesizing powders. Mechanical alloying shows a great potential in the production of nanostructured intermetallic powders. Mechanical alloying is conducted at room temperature and therefore it does not have defects, associated with melting and solidification [11–13]. Mechanical milling is associated with repeated collisions of powders with balls. During ball milling, deformation of powders, cold welding of particles, and particle fracture take place repeatedly and simultaneously. Mechanically alloyed powders can be consolidated with different techniques, including hot pressing, hot extrusion, injection molding, and spark plasma sintering (SPS). The latter is based on the sintering of powders under external pressure, together with using a high pulsed electric current, which goes directly through compacted powders [14–16]. Application of electrical current and generation of sparks during sintering enhance the diffusion kinetics of alloying elements. Compared to more traditional sintering techniques, spark plasma sintering is known to be a comparatively faster method with a very short sintering time. As well, spark plasma sintering is conducted at lower temperatures in comparison to conventional sintering methods. This characteristic is of great importance in case grain growth during sintering is a major concern. Low sintering temperature and short consolidation time minimize the risk of excessive grain growth, and this in turn means that spark plasma sintered parts potentially have much better mechanical properties [17].

* Corresponding author.
E-mail address: m.yazdanmehr@tudelft.nl (M.Y. Mehr).

https://doi.org/10.1016/j.mtcomm.2018.09.002
Received 20 August 2018; Received in revised form 31 August 2018; Accepted 3 September 2018
Available online 05 September 2018

This paper aims at studying microstructure and mechanical properties of Ni_3Al- xB (x = 0.5, 1.0, and 1.5 at%) samples, made by mechanical allotting and spark plasma sintering. There are several studies on the influences of boron on the mechanical properties of Ni_3Al compound [18,19]. But, results are not consistent and it is not easy to make a definitive conclusion on the effects of boron. This paper tries to present a systematic study of the effects of boron on the microstructure and mechanical properties of mechanically alloyed and spark plasma sintered Ni_3Al alloy. This paper is to our knowledge the only systematic study on the spark plasma sintering of this intermetallic.

2. Materials and methods

Ni (99.9% purity, 3 μm average size), Al (99.9% purity, 22 μm average size) and B (99.5% Purity, 2 μm average size) powders were used to synthesize Ni_3Al- xB (x = 0.0, 0.5, 1.0, and 1.5 at%) compound. Alloying was conducted with mechanical milling under argon atmosphere at room temperature. Stearic acid was added to the powder mixture to prevent sticking of powders to the balls or the chamber. All milling experiments were performed with a constant rotation speed of 350 rpm and ball-to-powder ratio 10:1. A combination of balls with different diameters were used for milling; 4 balls with 20 mm diameter, 3 balls with 12 mm diameter and 2 balls with 10 mm diameter. Sampling for microstructural characterization was done by interrupting the milling at every 10 h. X-ray diffractometer (XRD, Philips, Cu kα radiation, λ = 0.1541 nm) analysis was used to investigate the phase transformation in powders. Besides, average grain size was measured from XRD patterns, using Scherrer formula, as given below [20]:

$$D = \frac{0.9\lambda}{\beta(2\theta)Cos\theta} \quad (1)$$

where $\beta(2\theta)$ is the full width at half maximum (FWHM) of XRD peaks at diffraction angle θ, λ is the wavelength of the incident beam, and D is the crystallite size. As well, the lattice strain (ε) was calculated, using Wilson equation, given below [20]:

$$\varepsilon = \frac{\beta(2\theta)}{2\tan\theta} \quad (2)$$

Broadening of XRD peaks during milling has contributions from both grain refinement and lattice strain. The effects of the former is more pronounced at low angle diffraction peaks, whereas the latter has more effects on the broadening of high angle peaks [9–21]. Therefore, it is more accurate to use low angle reflections (i.e. (1 1 1) and (2 0 0) peaks) to calculate the average crystallite size, and high angle peaks (i.e. (2 2 0) and (3 1 1) peaks for Ni, and (2 2 0) and (3 1 1) peaks for Ni_3Al compound) to calculate lattice strains. Changes in the morphology of the powders during milling was evaluated by scanning electron microscope (SEM). Energy dispersive X-ray spectroscopy (EDS) point analysis and mapping were used for elemental analyses. Synthesized powders were consolidated by "KPF vacuum technology" SPS equipment, to obtain samples with diameter 1.5 mm and thickness 0.8 mm. Spark plasma sintering was conducted by compressing powders in a graphite die with uniaxial pressure 50 MPa using a hydraulic press. Sintering was performed at 950 °C, with holding 10 min holding time. The heating rate to reach sintering temperature was 150 °C min^{-1}. The microstructure of sintered specimens was evaluated using SEM and optical microscope. As well, the amount of porosities in sintered samples were estimated with an image analyzer. Mechanical properties of bulk specimens were evaluated using shear punch and Vickers micro-hardness tests (with 0.1 kg force). The shear punch was done with a punch with diameter 3 mm. The fractorgraphy of punched specimens was conducted as well.

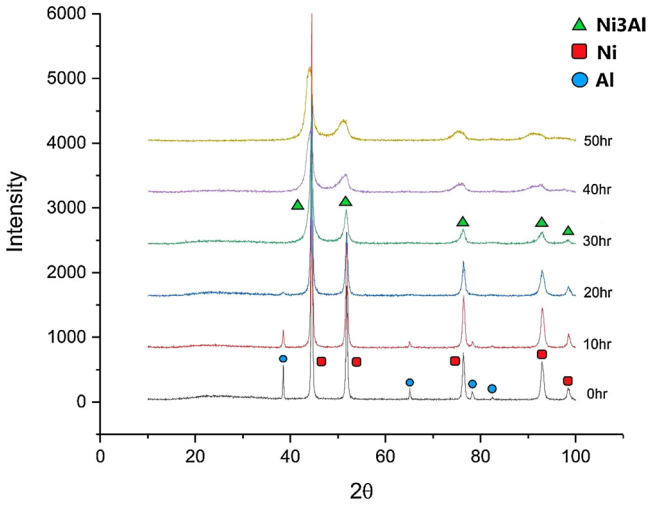

Fig. 1. XRD spectra of Ni and Al powder mixture with milling time.

3. Results

3.1. Synthesis and characterization of Ni_3Al compound

The effects of milling time on the XRD spectra of mechanically alloyed Ni_3Al powder mixture are shown in Fig. 1. Results show that intensities of Ni and Al peaks decrease with milling time. The decrease in the intensity of XRD peaks is associated with peak broadening and peak shift towards lower angles. The intermetallic compound has formed at 30 h. Fig. 2 shows elemental mapping of a particle after 30 h of milling. Elemental mapping gives an overview of distribution of alloying elements in the matrix. Al and Ni elements in this case are to a great extent homogeneously mixed, such a way and there is hardly any sign Al or Ni agglomeration. Milling in this investigation was continued till 50 h to make sure that alloying is completely done all over the sample.

Fig. 3 shows the evolution of the morphology of powders during milling. In 0 h time, Al particles with smaller size and Ni powders with greater size are mixed together. After 10 h of milling, Ni powders are fractured and size distribution is more homogenous. Ni powders are bigger and this will increase the probability of ball-powder collision, and this in turn results in a relatively faster fragmentation of Ni powders. One can also see agglomerated spots and intermingling of Ni and Al particles. At this stage cold welding and diffusion of alloying elements are expected to take place [22]. Excessive localized plastic deformation induced by ball-powder collisions and the fact that both Al and Ni have great formability result in the formation of plate-like particles. Particles have become completely plate-like after 20 h of milling (see Fig. 3c). Further milling leads to the transformation of plate-like morphology to the spherical morphology, which is due to the fragmentation of cold-deformed work-hardened plate-like particles, such a way that at 30 h milled powder mixture there is hardly any plate-like particle left. The morphology of particles does not change much from this point on. The only thing which can be noticed is the coarsening of particles with milling time. The average size of particles after 50 h of milling is almost three times bigger than that of 30 h milled sample. Cold welding, inter-diffusion of alloying elements, and tendency to decrease surface to volume ratio are reasons of particle growth during milling.

Fig. 4 shows the evolution of crystallite size as well as lattice strain during milling. Results show that first 10 h of milling does not change the crystallite size and lattice strain of Ni and Al powders. The dominant phenomenon at this early stage is the fragmentation of powders. Further milling up to 20 h is associated with a decrease in the grain sizes of Ni and Al elements down to 20 nm and 15 nm respectively.

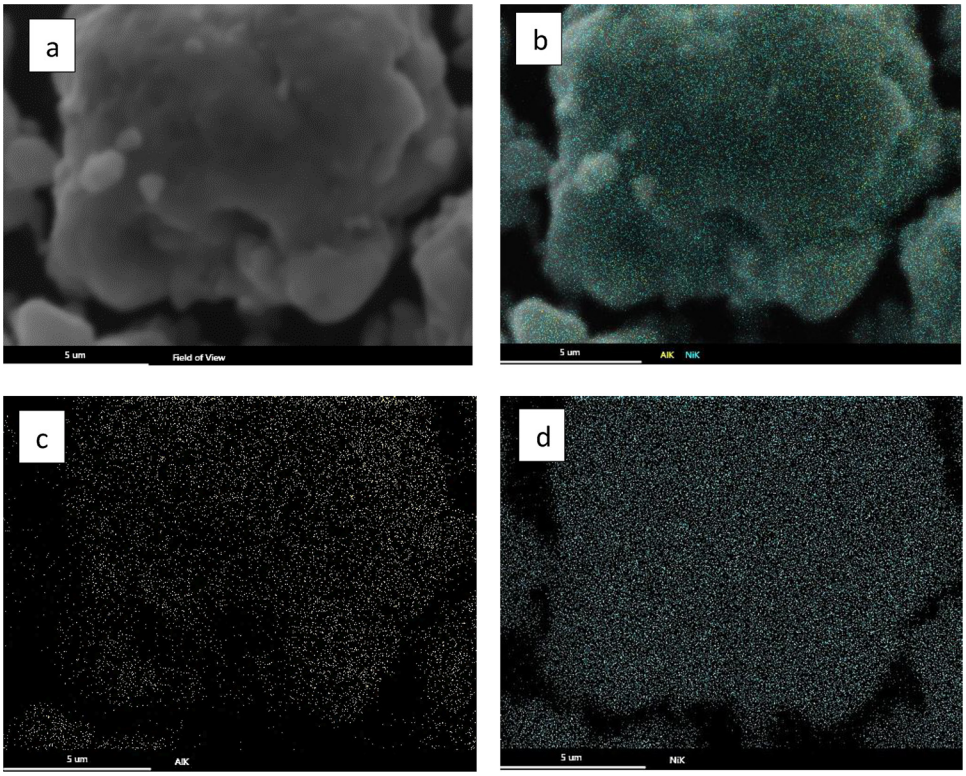

Fig. 2. Elemental mapping of a particle after 30 h of milling; a) SEM image, b) overlay of image and elemental analysis, c) distribution of Al, and d) distribution of Ni.

Further milling up to 30 h, as mentioned earlier, results in the formation of Ni_3Al intermetallic compound. Both crystallite size and lattice strain of 30 h milled Ni_3Al compound are comparable to those of Ni at the end of its stability (i.e. after 20 h milling). This implies that Ni is the host element, and Al is the one which diffuses into the crystal structure of Ni. Additional milling of Ni_3Al compound results in a slight decrease of grain size from 20 nm to 16 nm, followed by an increase up to 18 nm. Given that the minimum grain size was achieved after 40 h of milling, milling time for boron-containing samples was chosen to be 40 h.

3.2. Synthesis and characterization of Ni_3Al-xB ($0 < x < 1.5$ at%) compounds

Boron-containing samples were also synthesized in this study, with B ranging from 0.5 to 1.5 at%. Boron addition does not seem to have a major influence on the morphology of mechanically alloyed powders. Fig. 5 shows two examples of comparison between powder morphologies of Ni_3Al with and without B. Hardly is there any difference between morphologies in these two cases. Boron addition, however, alters the crystallite size and lattice strain (See Fig. 6). Overall B tends to decrease grain size and increase the lattice strain. The effect of B on both crystallite size and lattice strain is not huge though. In case of crystallite size, for example, the maximum B-induced reduction of crystallite size is only in the order of 5 nm. This applies to lattice strain as well, where the increase in lattice strain due to B addition does not exceed 0.1.

3.3. Consolidation of powders

Figs. 7 and 8 show porosity percentages of the consolidated specimens. It appears that addition of B enhances the sintering response of the powder mixture. The higher the B content, the lower the porosity content of the consolidated sample is. This effect is more pronounced, when the B content is higher than 1.0 at%. Boron is an interstitial alloying element, which obviously enters into the lattice structure of Ni_3Al. This is accompanied with the distortion of the lattice structure, resulting in an easier diffusion of alloying elements at the interface of particles during sintering. Easier diffusion of alloying elements obviously means faster and more effective sintering. There is not much difference between the porosity percentages of the samples with 1.0 and 1.5 at% of boron, with both specimens having almost similar porosity percentage of roughly 5%.

3.4. Mechanical properties of Ni_3Al-xB ($0 < x < 1.5$ at%) compounds

Fig. 9 shows the hardness of spark plasma sintered samples. Results depict that B-free and Ni_3Al-0.5at%B samples have almost similar hardness. This is also the case for Ni_3Al-1.0at%B and Ni_3Al-1.5at%B samples. Boron addition up to 0.5 at% does not significantly alter hardness of Ni_3Al intermetallic compound. This also applies to the case when B content is higher than 1.0 at%. It appears that B addition is influential the most when B content is 1.0 at%.

Fig. 10 shows the effects of B addition on the mechanical properties of Ni_3Al-xB ($0 < x < 1.5$at%) alloys in shear punch test. Interestingly, general outline is similar to what is seen in Fig. 9, i.e. shear punch test results for the B-free and Ni_3Al-0.5at%B samples are very similar and close together and the same goes for other two samples of higher B contents.

Fig. 11 shows fracture surfaces of alloys Ni_3Al and Ni_3Al-1.0at%B. There is no indication of transformation of fracture mode from brittle intergranular to the ductile transgranular mode with 1.0 at% boron addition. Bumps and dimples on the fracture surface of the alloy Ni_3Al has obviously to do with the high percentage of porosity in this sample.

4. Discussion

This papers investigates the effects of mechanical alloying and spark plasma sintering on the structure and mechanical Ni_3Al-xB ($0.0 < x < 1.5$ at%) intermetallic alloy. Powders during mechanical alloying experience repeated excessive local deformation, followed by

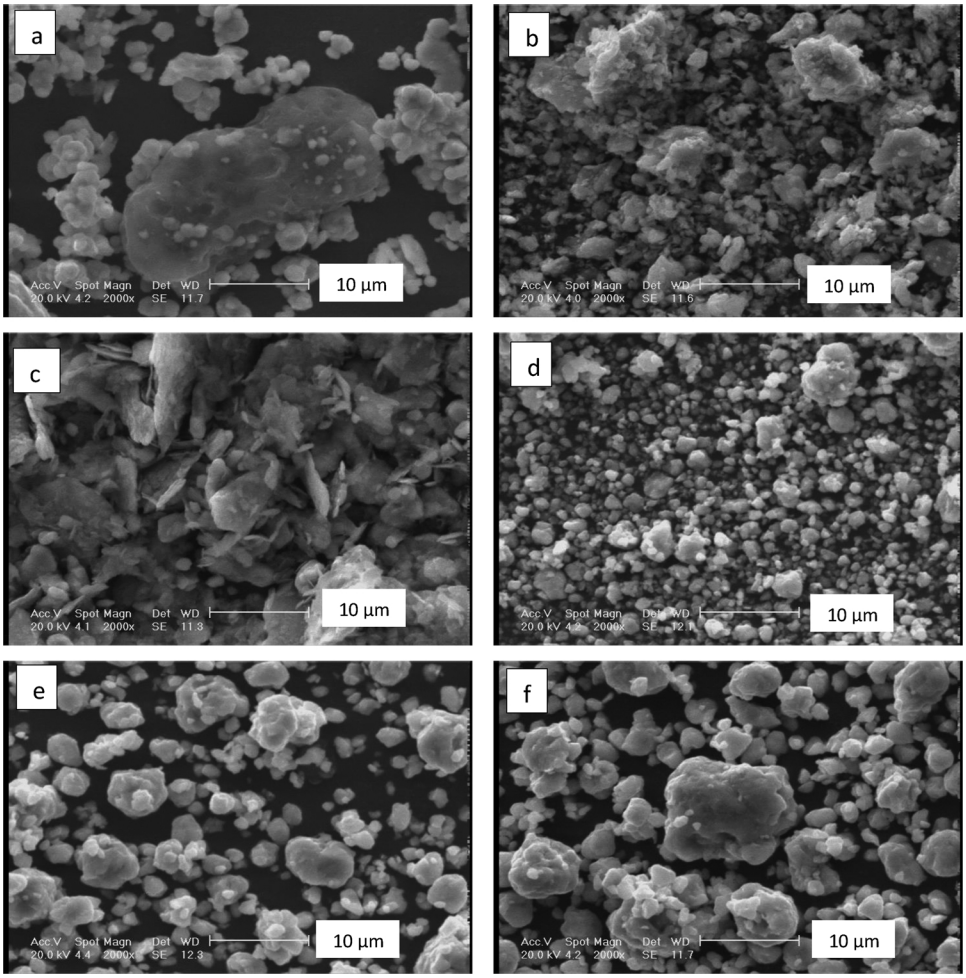

Fig. 3. SEM images of the evolution of the morphology of milled powders after for a) 0 h b) 10 h, c) 20 h, d) 30 h, e) 40 h, and f) 50 h.

local interfacial temperature increase. This results in the inter-diffusion of alloying elements and displacement of atoms from their equilibrium lattice sites. Alloying elements tend to diffuse towards certain atomic sites in the superlattice structure. In case of mechanical alloying of Ni and Al powder mixtures, early stage of milling is reportedly associated with the diffusion of Al into the Ni lattice structure, resulting in the formation of Ni-Al solid solution. The reason Al diffuses into Ni matrix has to do with the fact that diffusion of Al is comparatively faster [4]. Results in this study showed that further milling up to 30 h leads to the transformation of Ni-Al solid solution to Ni_3Al compound. Abbasi et al. [4] and Enayati et al. [10] also reported that Ni_3Al compound has formed after 20 h of milling. Further milling decreases the crystallite size of Ni_3Al alloy and causes lattice distortion. As well, one can notice that the change from 20 h to 40 h of milling is much more pronounced than that observed from 40 to 50 h. This implies that microstructure has reached a stable state after 40 h of milling. Further milling does not make a significant difference in the characteristics of synthesized powders. The observed shift towards left, which is an indication that lattice parameter has increased, is to be expected given that the solute (in this case Al) is larger than the solvent (Ni), with the former being 1.43 A and the latter 1.24 A. The kinetics of grain size decrease at early stages of milling is much faster in Al, compared to Ni, which implies that Al is plastically more deformable. This is also the case in lattice strain, where the kinetics of strain accumulation in Al is considerably

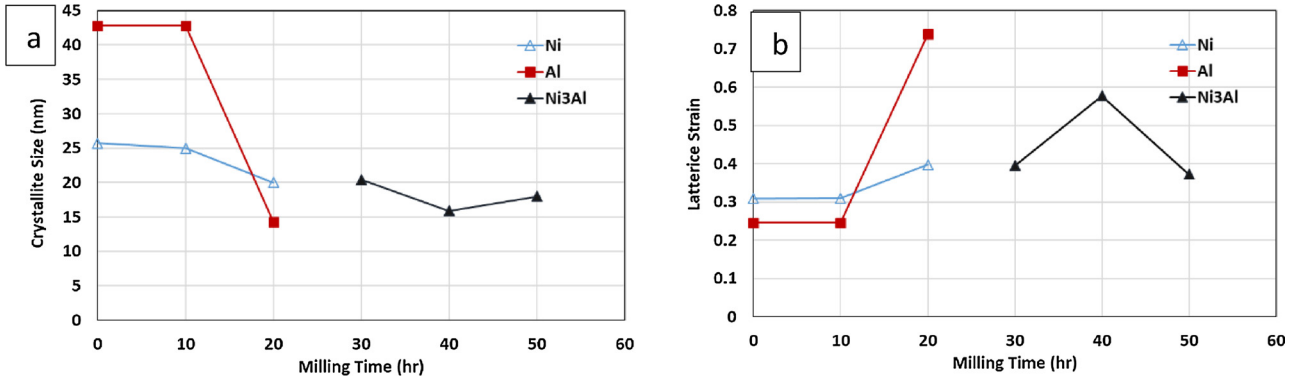

Fig. 4. Effects of milling time on the a) crystallite size and b) lattice strain of powders.

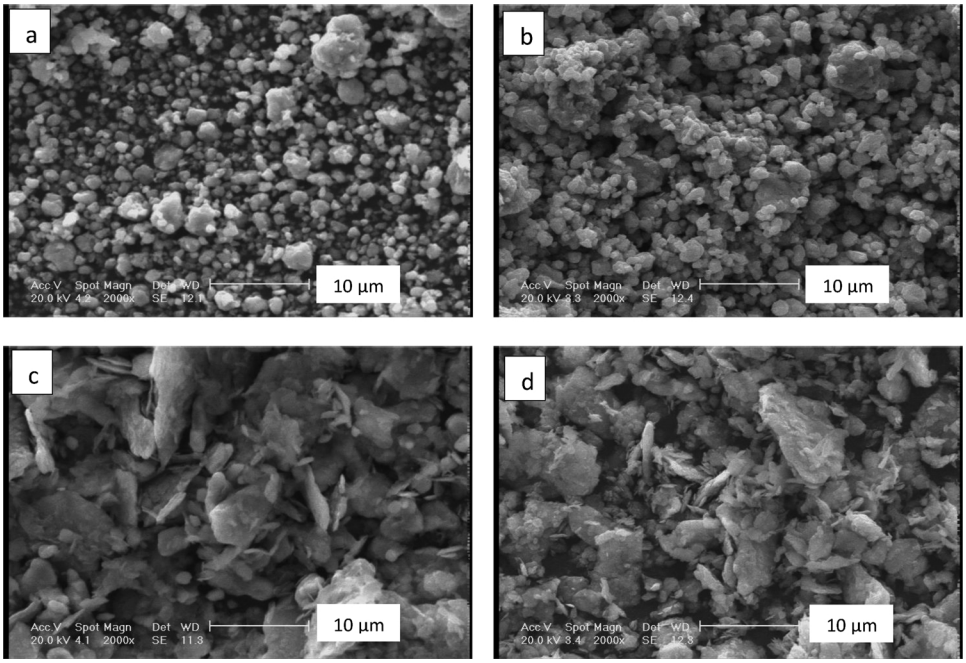

Fig. 5. Comparison between the morphologies of Ni_3Al particles, with and without B; a) Ni_3Al 30 h, b) Ni_3Al-1at%B 30 h, c) Ni_3Al 20 h, d) Ni_3Al-0.5at%B 20 h.

higher than that in Ni. While the lattice strain in Ni after 20 h of milling is almost 0.4, that in the Al is almost 0.75. Milling of Ni_3Al compound up to 40 h also results in grain refinement down to 16 nm, followed by an increase to 18 nm with further milling up to 50 h. The observed increase at the very late stage of milling is possibly due to the competition between grain refinement due to ball/powder collisions and grain growth due to localized temperature increase at the ball/powders interface. This obviously is the case in the lattice strain as well, with the final reduction being due to a thermal-induced strain relief.

Boron, when added to Ni_3Al, decreases the crystallite size. As well, boron-containing samples, when sintered, have comparatively lower porosity percentages. B is an interstitial alloying element which obviously enters into the lattice structure of Ni_3Al. This is accompanied with the distortion of the lattice structure, resulting in an easier diffusion of alloying elements at the interface of particles during sintering. Easier diffusion of alloying elements obviously means faster and more effective sintering. Boron exhibits a large solid solution strengthening effect in Ni_3Al [23]. This solid solution strengthening, combined with large lattice strain, caused by entering B into the lattice structure results in the observed improvement of hardness [24]. Also, B partly segregates into grain boundaries, and this in turn improves the grain boundary cohesive strength [25]. B segregation to grain boundaries will have significant implications for the mobility and accumulation of dislocations behind grain boundaries [26]. Results of shear punch test show that B additions higher than 0.5 at% results in a significant deterioration of ductility. Existing literature on the effects of B on the ductility of Ni_3Al alloy is quite controversial [27–31]. Aoki et al. [27] reported that small additions of B can significantly enhance the ductility of Ni_3Al. This positive B effect is more reported in solidified and recrystallized alloys though [28,29]. Several mechanisms are proposed so far, with most being based on the B-induced grain refinement as well as B-induced decrease of order intermetallic phase at grain boundaries, which is associated with higher degree of dislocation mobility [32]. On the contrary, it is postulated that the positive influence of boron on the ductility of Ni_3A1 can only be achieved when boron is in solid solution [26]. This possibly has to do with the fact that crack propagation takes place through grain boundaries. In fact, grain boundary failure is believed to be the main reason for observed brittleness in Ni_3Al alloy, no matter how many slip systems are active within the bulk of the alloy [26]. To resolve this controversy, one needs to bear in mind that to our knowledge all studies on the effects of boron on the ductility of Ni_3A1alloys focus on cast polycrystalline and single crystal materials. In this case, sintered specimens are largely deformed nanostructured materials, with grain boundaries being a dominant and controlling factor. The increase or decrease in the ductility is due to a combination of the bulk and grain boundary effects as well as combination of

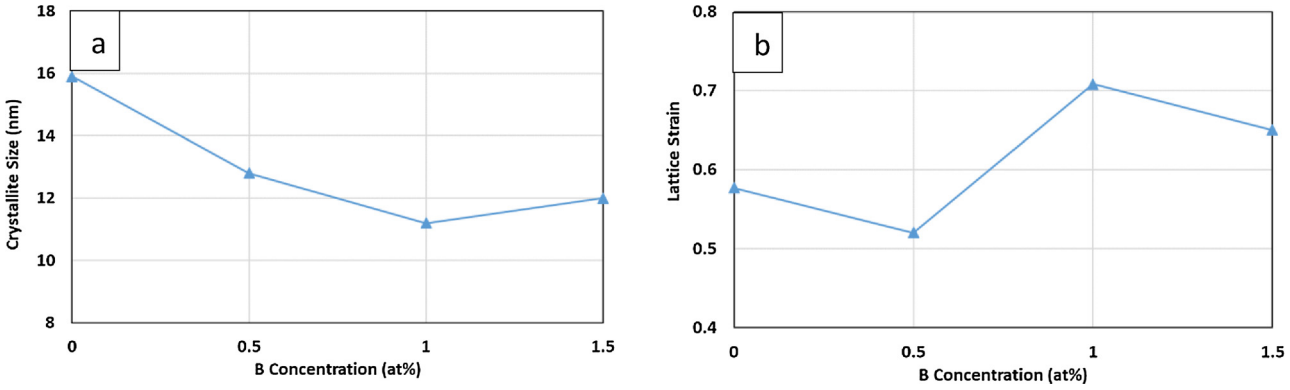

Fig. 6. Effects of B addition on the a) crystallite size and b) lattice strain of Ni_3Al compound, milled for 40 h.

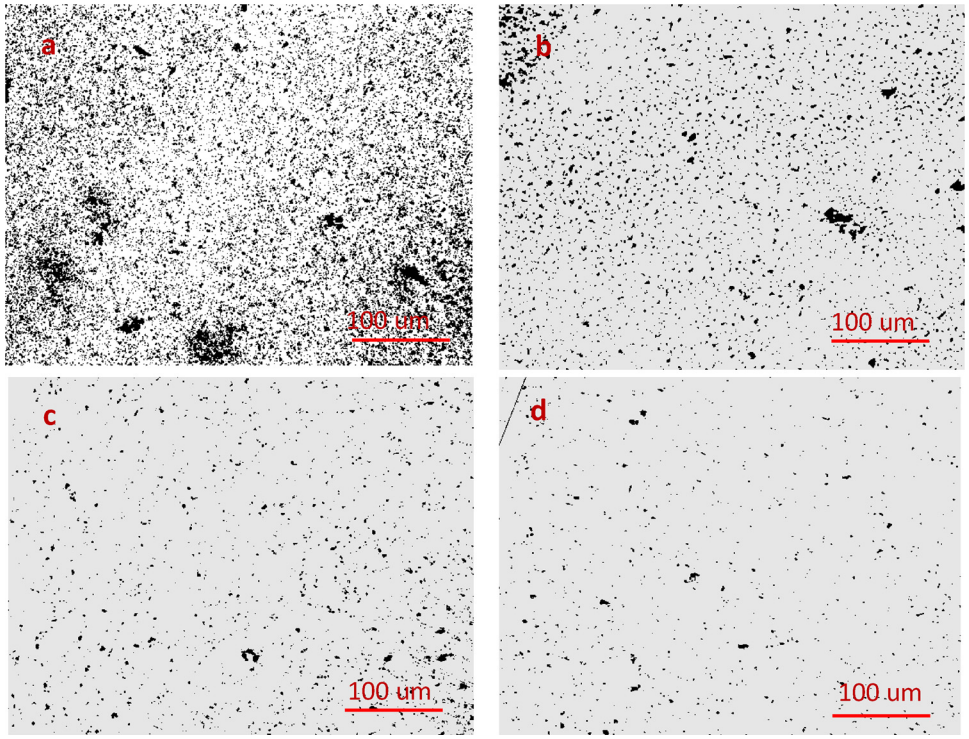

Fig. 7. Effects of B addition on the porosity size percentage and distribution in consolidated samples.

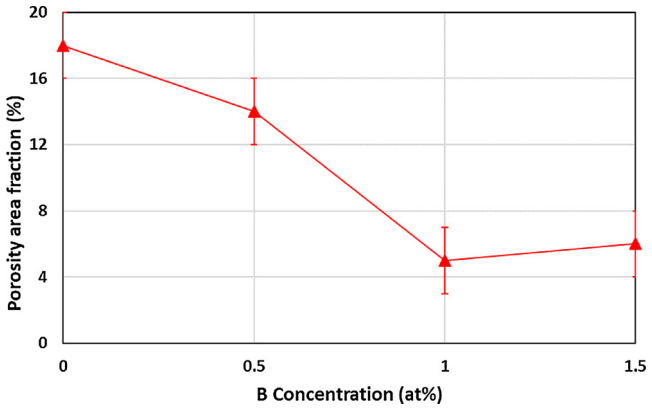

Fig. 8. Effects of B addition on the porosity percentage of consolidated samples.

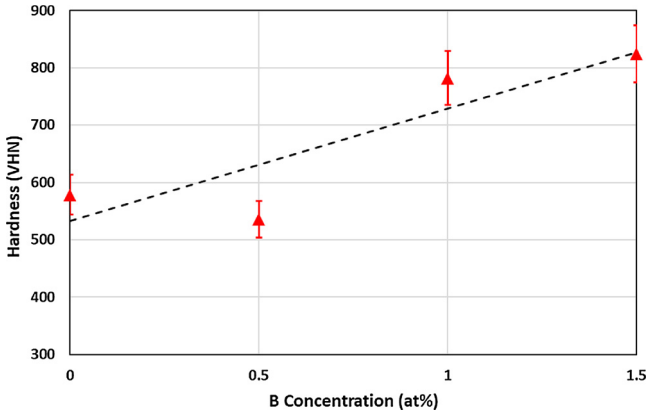

Fig. 9. Effects of Boron addition on the hardness of sintered Ni_3Al-xB ($0 < x < 1.5$at%) alloys.

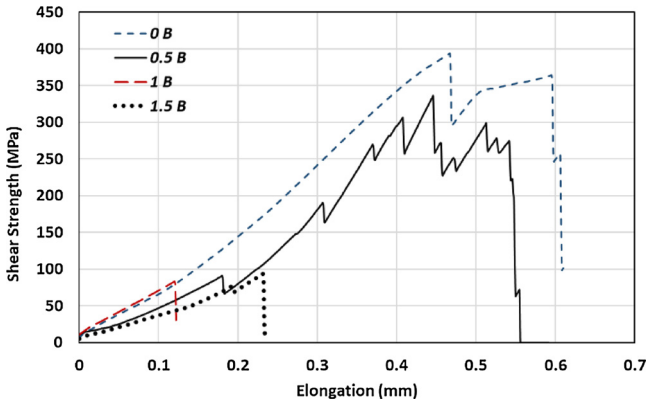

Fig. 10. Effects of boron addition on the stress-strain of sintered Ni_3Al-xB ($0 < x < 1.5$at%) alloys (The serrations in curves are due to the formation micro-cracks).

different mechanisms, including preferred crack propagation through grain boundaries, grain refinement, and the formation of disorder regions in the vicinity of grain boundaries.

5. Conclusions

This paper investigates the synthesis and characterization of Ni_3Al-xB ($0.0 < x < 1.5$ at%) alloy, using mechanical alloying (MA) and spark plasma sintering (SPS). Based on the results, obtained in this study, the following conclusions can be drawn:

- Ni_3Al compound can be synthesized with 30 h of milling, in a planetary ball mill with the rotation speed of 350 rpm and ball-to-powder ratio 10:1.
- Milling is associated with a significant grain refinement and accumulation of lattice strains. Powders with crystallite size lower than 20 nm can be synthesized with 30 h of milling. Grain refinement and strain accumulation in powdered samples reflect itself in XRD

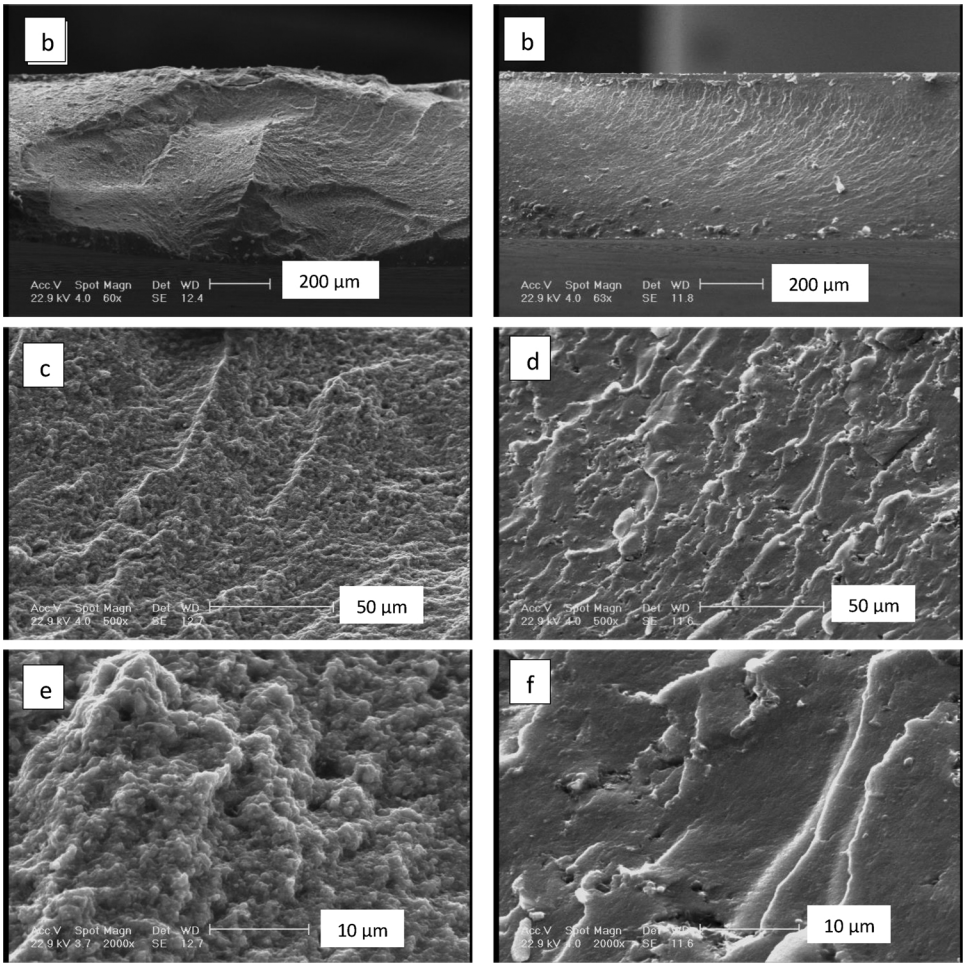

Fig. 11. Shear punch fracture surface of a,c,e) Ni_3Al and b,d,f) Ni_3Al-1at%B alloys in different magnifications.

spectra by peak broadening and shifts in the peak positions.

- Milling up to 20 h is associated with the formation of plate-like particles. Further milling results in the transformation of plate-like particles to rounded particles due to the repeated fragmentation of cold-deformed work-hardened plate-like particles.
- Boron addition overall reduces crystallite size and increases the lattice strain of mechanically alloyed powders.
- Boron also enhances the sintering response of the powders. The higher the boron content, the lower is the porosity percentage in the sintered samples.
- Boron additions between 0.5 and 1.0 at% leads to a significant increase in shear strength and hardness and a drop in the ductility of Ni_3Al-xB ($0.0 < x < 1.5$ at%) alloy. Boron addition over 1.0 at% does not result is a significant alteration of mechanical properties.

References

[1] K. Bochenek, M. Basista, Advances in processing of NiAl intermetallic alloys and composites for high temperature aerospace applications, Prog. Aerosp. Sci. 79 (2015) 136–146.
[2] V.K. Sikka, M.L. Santella, J.E. Orth, Processing and operating experience of Ni_3Al-based intermetallic alloy IC-221M, Mater. Sci. Eng. A 239–240 (1997) 564–569.
[3] V.K. Sikka, S.C. Deevi, S. Viswanathan, R.W. Swindeman, M.L. Santella, Advances in processing of Ni_3Al-based intermetallics and applications, Intermetallics 8 (2000) 1329–1337.
[4] M. Abbasi, S.A. Sajjadi, M. Azadbeh, An investigation on the variations occurring during Ni_3Al powder formation by mechanical alloying technique, J. Alloys Compd. 497 (2010) 171–175.
[5] K. Aoki, O. Izumi, Ductility and fracture behavior of B-doped polycrystalline Ni_3Al, J. Japan Inst. Met. 43 (1979) 1190–1194.
[6] J. Meng, C. Jia, Q. He, Effect of mechanical alloying on the structure and property of Ni_3Al fabricated by hot pressing, J. Alloys Compd. 421 (2006) 200–203.
[7] L. Lu, M.O. Lai, S. Zhang, Evolution and characterization of a Ni3Al intermetallic compound during mechanical alloying, Mater. Des. 15-2 (1994) 79–86.
[8] A. Antolak-Dudka, M. Krasnowski, S. Gierlotka, T. Kulik, Nanocrystalline Ni_3Al-based alloys obtained by recycling of aluminium scraps via mechanical alloying and consolidation, Adv. Powder Technol. 27 (2016) 305–311.
[9] Y. Yu, J. Zhou, J. Chen, H. Zhou, C. Guo, B. Guo, Synthesis of nanocrystalline Ni_3Al by mechanical alloying and its microstructural characterization, J. Alloys Compd. 498 (2010) 107–112.
[10] M.H. Enayati, Z. Sadeghian, M. Salehi, A. Saidi, The effect of milling parameters on the synthesis of Ni_3Al intermetallic compound by mechanical alloying, Mater. Sci. Eng. A 375–377 (2004) 809–811.
[11] C. Suryanarayana, Mechanical alloying and milling, Prog. Mater. Sci. 46 (1–2) (2001) 1–184.
[12] C. Suryanarayana, N. Al-Aqeeli, Mechanically alloyed nanocomposites, Prog. Mater. Sci. 58-4 (2013) 383–502.
[13] C. Suryanarayana, Synthesis of nanocomposites by mechanical alloying, J. Alloys Compd. 509 (Suppl. (1)) (2011) S229–S234.
[14] L. Cao, Wang Z, Z. Yin, K. Liu, J. Yuan, Investigation on mechanical properties and microstructure of silicon nitride ceramics fabricated by spark plasma sintering, Mater. Sci. Eng. A 731 (25) (2018) 595–602.
[15] V.N. Chuvildeev, D.V. Panov, M.S. Boldin, A.V. Nokhrina, Y.V. Blagoveshchensky, N.V. Sakharova, S.V. Shotin, D.N. Kotkov, Structure and properties of advanced materials obtained by spark plasma sintering, Acta Astronaut. 109 (2015) 172–176.
[16] M. Tokita, Development of hardware and software for spark plasma sintering (SPS) technology, J. High Temp. Soc. Japan 31 (2005) 215–224.
[17] V.N. Chuvildeev, M.S. Boldin, A.V. Nokhrin, A.A. Popov, Advanced materials obtained by spark plasma sintering, Acta Astronaut. 135 (2017) 192–197.
[18] M.L. Huang, C.Y. Wang, Effects of boron and carbon on the ideal strength of Ni solution and Ni_3Al intermetallics: a first-principles study of tensile deformation, Comput. Mater. Sci. 140 (2017) 140–147.
[19] N. Masahashi, Physical and mechanical properties in Ni_3A1 with and without boron, Mater. Sci. Eng. A223 (1997) 42–53.
[20] H.P. Klug, L.E. Alexander, X-ray Diffraction Procedures for Polycrystalline and Amorphous Materials, John Wiley and Sons, London, 1954.
[21] G.K. Williamson, W.H. Hall, X-ray line broadening from filed aluminium and wolfram, Acta Metall. 1 (1953) 22–31.
[22] A. Bahrami, H.R. Madaah Hosseini, P. Abachi, S. Miraghaei, Structural and soft

magnetic properties of nanocrystalline Fe85Si10Ni5 powders prepared by mechanical alloying, Mater. Lett. 60 (2006) 1068–1070.
[23] S.C. Huang, A.I. Taub, K.M. Chang, Boron extended solubility and strengthening potency in rapidly solidified Ni3Al, Acta Metall. 32 (1984) 1703–1707.
[24] N.F. Mott, F.R.N. Nabarro, Dislocation theory and transient creep, Conference on the Strength of Solids (1947) 1.
[25] C.T. Liu, C.L. White, Dynamic embrittlement of boron-doped Ni3Al alloys at 600°C, Acta Metall. 35 (1987) 643–649.
[26] F.E. Heredia, D.P. Pope, Effect of boron additions on the ductility and fracture behavior on Ni_3Al single crystals, Acta Metall. Mater. 39 (8) (1991) 2017–2026.
[27] K. Aoki, O. Izumi, Improvement of room temperature ductility by boron addition of L2 type intermetallic compound Ni_3Al, J. Japan Inst. Met. 43 (1979) 1190–1196.
[28] C.T. Liu, C.L. White, J.A. Horton, Effect of boron on grain-boundaries in Ni3Al, Acta Metall. 33 (1985) 213–229.
[29] A.I. Taub, S.C. Huang, K.M. Chang, Improved strength and ductility of Ni_3Al by boron modification and rapid solidification, Metall. Trans. A 15 (1984) 399–402.
[30] E.M. Schulson, T.P. Weihs, I. Baker, H.J. Frost, J.A. Horton, Grain boundary accommodation of slip in Ni_3Al containing boron, Acta Metall. 34 (1986) 1395–1399.
[31] E.P. George, C.T. Liu, D.P. Pope, Intrinsic ductility and environmental embrittlement of binary Ni_3Al, Scr. Metal. Mater. 28 (1993) 857–862.
[32] A.H. King, M.H. Yoo, High temperature ordered lntermetallic alloys, in: H.N.S. Stoloff, C.C. Koch, C.T. Liu, O. Izumi (Eds.), Materials Research Society Symposia Proceedings, vol. 81, Materials Research Society, Pittsburgh, 1987, pp. 45–53.